Materials Research Proceedings 33 (2023) 219-225 https://doi.org/10.21741/9781644902677-32

Development of accurate fluid-structure interaction models for aerospace problems

Andrea Rubino[1,a *], Marco Donato de Tullio[1], Dario De Marinis[1], Maria Cinefra[1]

[1]Polythecnic of Bari, Italy

[a]andrea.rubino@poliba.it

Keywords: Fluid-Structure Interaction, Finite Element Method, Carrera Unified Formulation, Adaptive Mesh

Abstract. The research program deals with fluid-structure interaction (FSI), a challenging field of engineering, with a practical application on aerospace problems such as the flutter, an instability problem due to aeroelastic excitations. The research goal is to find a suitable way to deal with flutter in such a way the two macro fields, fluid and structure, are modelled with mid to high-level accuracy. Moreover, the creation of an interface could be useful to study other problems, such as the cabin comfort for an aircraft. To do that, the research activity is firstly split in two to study in depth the structural and the fluid problem, then they are merged together through the interface analysis: the main problem is that each field has an own scale and the union of both requests a suitable modelling and analysis. After a preliminary study on the state of the art of fluid-structure interaction in literature, which forms the pillar of the research project, the structural field is analysed first. The study of the structure system is carried out on the Carrera Unified Formulation (CUF), which allows a reduced degrees of freedom model with the same accuracy of the classical Finite Element Method (FEM). Analysis on possible adaptive mesh methods is needed in order to match the proper scale at interface with fluid dynamics system. This work could be a milestone for future investigation in problems that need a mesh refinement, beyond the aeroelastic field. Then, the fluid system is studied and analysed through the Navier-Stokes equations. In particular, a Dual Time Stepping model for non-stationary Favre Average Navier-Stokes is used. More in general, considering different order of magnitude for the Reynold's number, three different analysis could be done: Reynolds Average Navier-Stokes (RANS) for only large-scale eddies resolved and other components modelled, Large Eddy Simulation (LES) which adds the resolution of the flux of energy with respect to the previous simulation and Direct Numerical Simulation (DNS) which resolves also the dissipating eddies, so representing the best performing simulation but with very high computational cost. Finally, a complete simulation of fluid-structure interaction is performed to find the flutter velocity and study the induced vibrations from turbulent boundary layer to the aircraft cabin and/or to the rocket nose.

State of the art

The state of the art for an accurate fluid-structure interaction model is the following: considering commercial codes and analysing the literature, there is a large number of models where the fluid part is accurate and studied in depth and the structural part is dealt in a simpler manner, or there is a considerable number of models in which the situation is reversed, so the structural part is deepened and the fluid part is approximated with less accuracy. The problem is not simple to deal with, because different scales are involved and combining them is a challenging process, as ell indicated in Fig. 1.

Materials Research Proceedings 33 (2023) 219-225 https://doi.org/10.21741/9781644902677-32

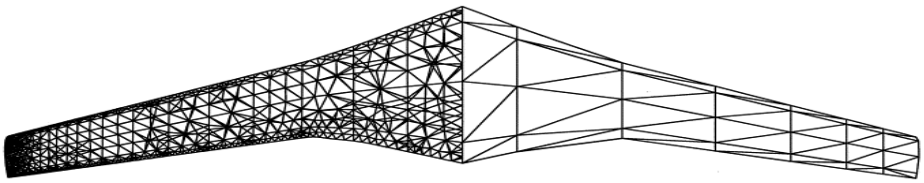

Fig. 1 – Fluid vs. Structural modelling. Credits: CCTech®

In particular, several cases are present in the literature, distinguishing between the models used: linear and non-linear. Among the former, we mention the Classical Aerodynamic Theory (CAT), the Classical Hydrodynamic Stability Theory (CHST) [1], the Parallel Shear Flow with Dynamic Inviscid Perturbation (PSF with DIP) [2] and the Time-Linearized General Analysis (TLGA). Regarding non-linear models, the Harmonic Equilibrium Method (HEM) [3] and the System Identification Method (SIM) [4,5] are mentioned. These are added to the classic methods of studying the modes of vibration of the structure in the presence of external forces that simulate the effect of aerodynamic forces. What emerges from this first research is that there is a trend to widely use Reduced Order Models (ROMs) [6] to create a compromise between the number of degrees of freedom required by the fluid-structure interaction model and the available computational resources.

Methods of analysis

To develop an accurate FSI model, the idea is to use the Carrera Unified Formulation for the structural part and the Dual Time Stepping (DTS) model for non-stationary Favre Average Navier-Stokes for the fluid part.

Structural modelling - CUF

The choice on the CUF for the structural part is driven by several advantages: in fact, this formulation allows to describe the kinematic filed in unified manner, it allows to derive the governing equations in compact way and it gives accurate results with a low number of Degrees Of Freedom (DOFs). Let us consider a generic beam structure whose longitudinal axis, with respect to a Cartesian coordinate system, lays on the coordinate y, being its cross-section defined in the xz-plane. The displacement field of one-dimensional models in CUF framework is described as a generic expansion of the generalized displacements (in the case of displacement-based theories) by arbitrary functions of the cross-section coordinates:

$$\mathbf{u}(x,y,z) = F_{\tau}(x,z)\mathbf{u}_{\tau}(y) \qquad \tau = 1,\dots,M \tag{1}$$

where $u = \{u_x, u_y, u_z\}$ is the vector of 3D displacements and $u_\tau = \{u_{x\tau}, u_{y\tau}, u_{z\tau}\}$ is the vector of general displacements, *M* is the number of terms in the expansion, τ denotes summation and the functions $F_{\tau}(x,z)$ define the 1D model to be used. In the framework of plate theories, by considering the mid-plane of the plate laying in the xy-plane, CUF can be formulated in an analogous manner:

$$\mathbf{u}(x,y,z) = F_{\tau}(z)\mathbf{u}_{\tau}(x,y) \qquad \tau = 1,\dots,M \tag{2}$$

In the equation above, the generalized displacements are function of the mid-plane coordinates of the plate and the expansion is conducted in the thickness direction z. The main advantage of CUF is that it allows to write the governing equations and the related finite element arrays in a

Materials Research Proceedings 33 (2023) 219-225 https://doi.org/10.21741/9781644902677-32

compact and unified manner, which is formally an invariant with respect to the F_{τ} functions [7,8]. Let the 3D displacement vector be defined as:

$$\mathbf{u}(x,y,z) = \begin{cases} u_x(x,y,z) \\ u_y(x,y,z). \\ u_z(x,y,z) \end{cases} \tag{3}$$

According to classical elasticity, stress and strain tensors can be organized in six-term vectors with no lack of generality. They read, respectively:

$$\boldsymbol{\sigma}^T = \{\sigma_{yy} \ \sigma_{xx} \ \sigma_{zz} \ \sigma_{xz} \ \sigma_{yz} \ \sigma_{xy}\} \tag{4}$$

$$\boldsymbol{\varepsilon}^T = \{\varepsilon_{yy} \ \varepsilon_{xx} \ \varepsilon_{zz} \ \gamma_{xz} \ \gamma_{yz} \ \gamma_{xy}\} \tag{5}$$

Regarding to this expression, the geometrical relations between strains and displacements with the compact vectorial notation can be defined as:

$$\boldsymbol{\varepsilon} = \boldsymbol{Du} \tag{6}$$

where, in the case of small deformations and angles of rotations, D is the following linear differential operator:

$$D = \begin{bmatrix} 0 & \frac{\partial}{\partial y} & 0 \\ \frac{\partial}{\partial x} & 0 & 0 \\ 0 & 0 & \frac{\partial}{\partial z} \\ \frac{\partial}{\partial z} & 0 & \frac{\partial}{\partial x} \\ 0 & \frac{\partial}{\partial z} & \frac{\partial}{\partial y} \\ \frac{\partial}{\partial y} & \frac{\partial}{\partial x} & 0 \end{bmatrix} \tag{7}$$

On the other hand, or isotropic materials the relation between stresses and strains is obtained through the well-known Hooke's law:

$$\boldsymbol{\sigma} = \boldsymbol{C\varepsilon} \tag{8}$$

where **C** is the isotropic stiffness matrix:

$$C = \begin{bmatrix} C_{22} & C_{21} & C_{23} & 0 & 0 & 0 \\ C_{21} & C_{11} & C_{13} & 0 & 0 & 0 \\ C_{23} & C_{13} & C_{33} & 0 & 0 & 0 \\ 0 & 0 & 0 & C_{55} & 0 & 0 \\ 0 & 0 & 0 & 0 & C_{44} & 0 \\ 0 & 0 & 0 & 0 & 0 & C_{66} \end{bmatrix} \tag{9}$$

The coefficients of the stiffness matrix depend only on the Young's modulus, E, and the Poisson ratio, ν, and they are:

Materials Research Proceedings 33 (2023) 219-225 https://doi.org/10.21741/9781644902677-32

$$C_{11} = C_{22} = C_{33} = \frac{(1-\nu)E}{(1+\nu)(1-2\nu)}$$
$$C_{21} = C_{13} = C_{23} = \frac{\nu E}{(1+\nu)(1-2\nu)} \quad (10)$$
$$C_{44} = C_{55} = C_{66} = \frac{E}{2(1+\nu)}$$

In the case of 1D models, the discretization along the longitudinal axis of the beam is made by means of the finite element method. The generalized displacements are in this way described as functions of the unknown nodal vector, $\mathbf{q_{\tau i}}$, and the 1D shape functions, $N_i(y)$:

$$\mathbf{u_\tau}(y) = N_i(y)\mathbf{q_{\tau i}} \qquad i = 1, \dots, n_{elem} \quad (11)$$

where n_{elem} is the number of nodes per element and the unknown nodal vector is defined as:

$$\mathbf{q_{\tau i}} = \{q_{ux_{\tau i}} \quad q_{uy_{\tau i}} \quad q_{uz_{\tau i}}\}^T \quad (12)$$

Similarly, the FEM discretization of generalized displacements on the mid-surface of the plate can be written as follows:

$$\mathbf{u_\tau}(x,y) = N_i(x,y)\mathbf{q_{\tau i}} \qquad i = 1, \dots, n_{elem} \quad (13)$$

where 2D shape functions $N_i(x,y)$ are employed. Different sets of polynomials can be used to define FEM elements. Lagrange interpolating polynomials have been chosen in this work to generate both one-dimensional and two-dimensional elements. For the sake of brevity, their expression is not provided, but it can be found in the book by Carrera et. al [7], in which two-nodes (B2), three-nodes (B3) and four-nodes (B4) beam elements and four-nodes (Q4), nine-nodes (Q9) and sixteen-nodes (Q16) plate elements are described. By combining the FEM approximation with the kinematic assumptions of the Carrera Unified Formulation, the 3D displacement field can be written as:

$$\boldsymbol{u} = F_\tau N_i \mathbf{q_{\tau i}} \qquad i = 1, \dots, n_{elem} \quad (14)$$

where the functions F_τ and N_i are defined according to the type of element (beam or plate). Note that in Eq. 14 the shape functions N_i and the expanding functions F_τ are independent. A novel approach [9] is introduced considering a coupling by relating the expanding functions F_τ to the shape functions N_i by means of the following formalism:

$$\boldsymbol{u} = F_\tau^i N_i \mathbf{q_{\tau i}} \quad (15)$$

The difference of Eq. 15 from Eq. 14 is the additional superscript *i* of N_i, which is now an index also of the function F_τ. This definition introduces the dependency of the kinematic assumptions to the FE nodes, namely the Node-Dependent Kinematics (NDK) [10].

Fluid modelling - DTS

The choice on the DTS for non-stationary Favre Average Navier-Stokes for the fluid part is driven by the following considerations. The DTS scheme is similar to the approximate-Newton method, but has an additional sink term that can be controlled to optimize convergence. In fact, the iterative method is treated as a time-marching method based on a pseudo-time, and in this formulation, the physical-time derivative becomes a sink in the pseudo-time frame. The total system can be viewed as a steady-state calculation with a sink term dependent on the physical-time step. For large

Materials Research Proceedings 33 (2023) 219-225 https://doi.org/10.21741/9781644902677-32

physical-time steps, the sink term is small, the problem behaves like a steady-state problem and the Courant-Friedrichs-Lewy number based on the pseudo-time step (pseudo-CFL) should be set corresponding to the steady-state optimal values. For small time steps, the problem is sink dominated and the pseudo-CFL can be increased. Unlike the physical-time step, the pseudo-time step can be set locally depending on the local flow conditions and physical-time steps. The Reynolds Averaged Navier-Stokes (RANS) equations, in terms of Favre mass-averaged quantities, using the $k-\omega$ turbulence model, in a Cartesian coordinate system can be rewritten:

$$\frac{\partial \rho}{\partial t} + \frac{\partial}{\partial x_j}(\rho u_j) = 0 \tag{16}$$

$$\frac{\partial (\rho u_i)}{\partial t} + \frac{\partial}{\partial x_j}(\rho u_j u_i) = -\frac{\partial p_t}{\partial x_j} + \frac{\partial \hat{\tau}_{ji}}{\partial x_j} \tag{17}$$

$$\frac{\partial (\rho \tilde{H} - p_t)}{\partial t} + \frac{\partial}{\partial x_j}(\rho u_j \tilde{H}) = \frac{\partial}{\partial x_j}\left[u_i \hat{\tau}_{ji} + (\mu + \sigma^* \mu_t)\frac{\partial k}{\partial x_j} - q_j\right] \tag{18}$$

$$\frac{\partial (\rho k)}{\partial t} + \frac{\partial}{\partial x_j}(\rho u_j k) = S_k + \frac{\partial}{\partial x_j}\left[(\mu + \sigma^* \mu_t)\frac{\partial k}{\partial x_j}\right] \tag{19}$$

$$\frac{\partial (\rho \omega)}{\partial t} + \frac{\partial}{\partial x_j}(\rho u_j \omega) = S_\omega + \frac{\partial}{\partial x_j}\left[(\mu + \sigma \mu_t)\frac{\partial \omega}{\partial x_j}\right] \tag{20}$$

where

$$\tilde{H} = h + \frac{1}{2}(u^2 + v^2 + w^2) + \frac{5}{3}k \tag{21}$$

$$p_t = p + \frac{2}{3}\rho k = \rho R T + \frac{2}{3}\rho k = \rho\left(R + \frac{2k}{3T}\right) = \rho \tilde{R} T \tag{22}$$

$$S_k = \hat{\tau}_{ji}\frac{\partial u_i}{\partial x_j} - \beta^* \rho \omega k \tag{23}$$

$$S_\omega = \rho \alpha \frac{\omega}{k}\hat{\tau}_{ji}\frac{\partial u_i}{\partial x_j} - \beta \rho \omega^2 \tag{24}$$

and $\hat{\tau}_{ji}$ indicate the sum of the molecular and Reynolds stress tensor components:

$$\hat{\tau}_{ji} = (\mu + \mu_t)\left[\frac{\partial u_i}{\partial x_j} + \frac{\partial u_j}{\partial x_i} - \frac{2}{3}\frac{\partial u_k}{\partial x_k}\delta_{ij}\right] - \frac{2}{3}\rho k \delta_{ij} \tag{25}$$

The heat flux vector components q_j are rewritten as:

$$q_j = -\left(\frac{\mu}{Pr} + \frac{\mu_t}{Pr_t}\right)\frac{\partial h}{\partial x_j} \tag{26}$$

where Pr_t is the turbulent Prandtl number.

Innovation and significant results

In the first part of the PhD programme, the focus was on the structural modelling. In particular, the NDK approach was exploited to investigate the behaviour of simple geometries through static and dynamic analyses. These analyses are conducted using an academic code. Through the Node-Dependent Kinematic approach, a combination between mono- and bi-dimensional elements was

Materials Research Proceedings 33 (2023) 219-225 https://doi.org/10.21741/9781644902677-32

possible, obtaining a complete 3D field of displacements. The investigation highlighted the possibility to use *adapted* elements (see Fig. 3) to obtain *adaptive* meshing (see Fig. 2).

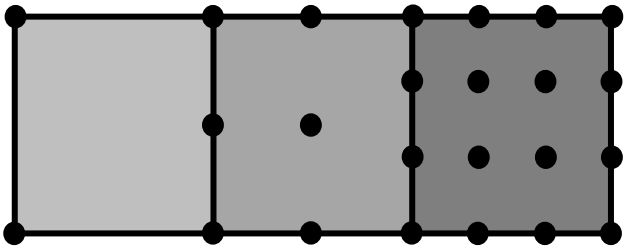

Fig. 2 – Adaptive meshing

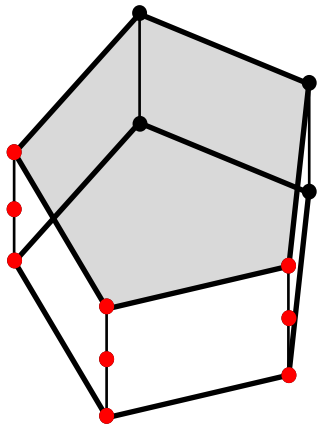

Fig. 3 – Adapted elements

Note that in Fig. 2 is possible to connect elements with different number of nodes using a combination of 1D and 2D elements, exploiting the CUF. Moreover, in Fig. 3 is highlighted the fact that the 3D element can be *distorted*, maintaining a different discretization along the thickness. Several benchmark problems are tested using these elements, showing results in accordance with those tabulated in literature or obtained with commercial codes (Patran/Nastran®). These are important achievements considering that the fluid-structure interface have to connect a finer mesh for fluid analysis with a coarse one for structural analysis (*adaptive* mesh), also in region with complicated geometries (*adapted* and *distorted* elements) [11].

Some important results are obtained considering a square plate with a concentrated load in the middle and a Razzaque's skew plate with a set of concentrated loads at the mid-line of the top surface. In Fig. 4 is reported an example of mesh and in Fig. 5 is shown a magnification of an element between two zones with different number of nodes.

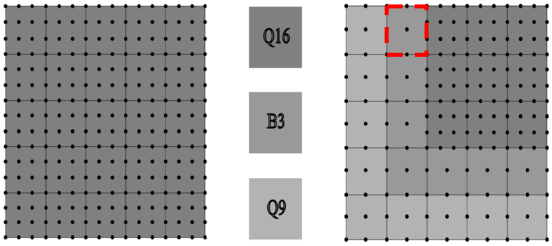

Fig. 4 – Square plate

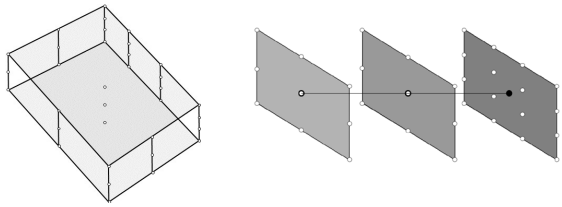

Fig. 5 – Adapted 1D element

The analysis with the reduced mesh allows to save DOFs:

Table 1 – Comparison between DOFs of full and reduced mesh

Square Plate	Razzaque's Plate
DOFs Full: 11532	DOFs Full: 7500
DOFs Reduced: 6600	DOFs Reduced: 4593
Saving: 42.77%	Saving: 38.76%

Moreover, different distorted meshes are analysed and compared in terms of displacements and frequencies, as shown in Fig. 6.

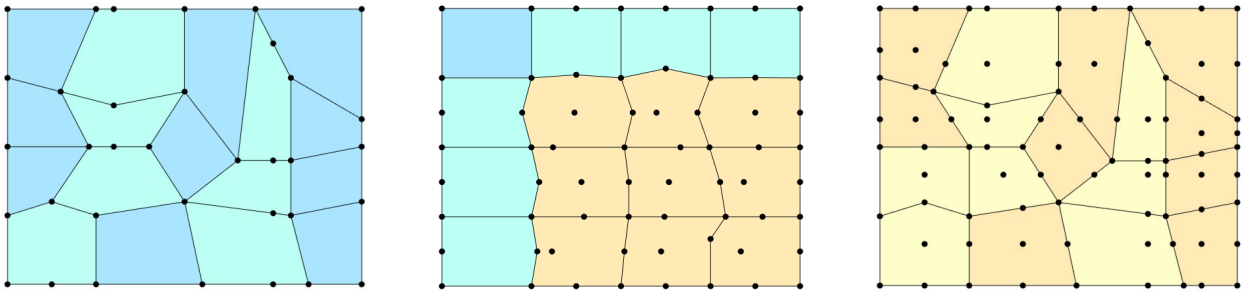

Fig. 6 – Different configurations of distorted meshes

In all the cases considered, the percentage errors are below the 1% almost always. The next steps are to implement the information exchange between the fluid part and the structural part.

Conclusion

In conclusion, the work done by far has demonstrated the potentiality of the method and represents an important milestone for the achievement of the final target: the development of accurate fluid-structure interaction models for aerospace problems.

References

[1] Lin CC. 1955. The Theory of Hydrodynamic Stability. Cambridge, UK: Cambridge, Univ. Press. 155 pp.
[2] Dowell EH. 1971. Generalized aerodynamic forces on a flexible plate undergoing transient motion in a shear flow with an application to panel flutter. AIAA. J. 9 (5):834-41 https://doi.org/10.2514/3.6283
[3] Hall KC, Thomas JP, Clark WS. 2000. Computation of unsteady nonlinear flows in cascades using a harmonic balance technique. Presented at the Int. Symp. on Unsteady Aerodyn., Aeroacoust. and Aeroelast. of Turbomach., 9th, Ecole Centrale de Lyon, Lyon, France, Sept. 4-7, 2000.
[4] Silva WA. 1993. Application of nonlinear systems theory to transonic unsteady aerodynamic responses. J. Aircraft 30(5):660-68 https://doi.org/10.2514/3.46395
[5] Silva WA. 1997. Discrete-time linear and nonlinear aerodynamic impulse responses for efficient (CFD) analyses. PhD thesis. Coll. William Mary. 159 pp.
[6] Dowell, E. H., & Hall, K. C. (2001). Modeling of fluid-structure interaction. Annual review of fluid mechanics, 33(1), 445-490. https://doi.org/10.1146/annurev.fluid.33.1.445
[7] Carrera, E., Giunta, G., Petrolo, M., 2011. Beam Structures: Classical and Advanced Theories. John Wiley and Sons, pp. 45-63. https://doi.org/10.1002/9781119978565
[8] Carrera, E., 2003. Theories and finite elements for multilayered plates and shells: a unified compact formulation with numerical assessment and benchmarking. Arch. Comput. Methods Eng. 10 (3), 216-296. https://doi.org/10.1007/BF02736224
[9] Carrera, E., Giunta, G., 2010. Refined beam theories based on Carrera's Unified Formulation. Int. J. Appl. Mech. 2 (1), 117-143. https://doi.org/10.1142/S1758825110000500
[10] Cinefra, M. (2021). Non-conventional 1d and 2d finite elements based on cuf for the analysis of non-orthogonal geometries. European Journal of Mechanics-A/Solids, 88, 104273. https://doi.org/10.1016/j.euromechsol.2021.104273
[11] Cinefra, M., & Rubino, A. (2022). Adaptive mesh using non-conventional 1D and 2D finite elements based on CUF. Mechanics of Advanced Materials and Structures, 1-11. https://doi.org/10.1080/15376494.2022.2126039